# Aerodynamic effect of icing/rain impacts on super-hydrophobic surfaces

**Okulova, Nastasia; Taboryski, Rafael J.; Sørensen, Jens Nørkær; Shtork, S. I.; Okulov, Valery**

*Published in:*
AIP Conference Proceedings

*Link to article, DOI:*
10.1063/1.5065139

*Publication date:*
2018

*Document Version*
Publisher's PDF, also known as Version of record

# Aerodynamic effect of icing/rain impacts on super-hydrophobic surfaces

N. Okulova, R. Taboryski, J. N. Sørensen, S. I. Shtork, and V. L. Okulov

Citation: AIP Conference Proceedings **2027**, 030045 (2018); doi: 10.1063/1.5065139
View online: https://doi.org/10.1063/1.5065139
View Table of Contents: http://aip.scitation.org/toc/apc/2027/1
Published by the American Institute of Physics

# Aerodynamic Effect of Icing/Rain Impacts on Super-Hydrophobic Surfaces

N. Okulova[1,2], R. Taboryski[2], J.N. Sørensen[3], S.I. Shtork[4], and V.L.Okulov[3,4 a)]

[1] *Danapak Flexibles A/S, 4200 Slagelse, Denmark*
[2]*Department of Micro- and Nanotechnology, Technical University of Denmark,* 2800 Kgs. Lyngby, Denmark
[3]*Department of Wind Energy, Technical University of Denmark, 2800 Kgs. Lyngby, Denmark*
[4]*Kutateladze Institute of Thermophysics, SB RAS. 630090, Novosibirsk, Russia*

[a)]Corresponding author: vaok@dtu.dk

**Abstract.** The rain impact and ice accretion on different aerodynamic constructions represent a large problem to their safety and operation. Most current de-icing systems include either physical or chemical removal of ice, which is resource- and energy-intensive as well as environmentally polluting. A more desirable approach to prevent initial ice formation from water droplets on a surface is to employ highly ordered super-hydrophobic materials, which mimic lotus leaves and other natural dirt- and water-repelling surfaces and reproduced in many laboratory tests. The ability to fend off water droplets could lead to prevention of icing as an inherent material property, which further would prevent ice formations, rather than fighting its build-up. Our objective is to draw attention to problems of an extension of this effect to technical applications. The main idea of the icing or rain protection of the different aerodynamic constructions may be the use of super-hydrophobic thermoplastic polymers with the water-repellent properties to prevent corrosion, improve aerodynamics or add self-cleaning properties to the material. The purpose of the present study is to explore the possibility of using a fast and cheap technology of R2R-EC to enable the fabrication of nanostructures on polymer foils of sizes ranging from 50 nanometers and up to 100 micrometers with the aim of improving the ice-cleaning and water-repellent properties of the coating. This high-speed and low-cost lithography method is developed at DTU and Danapak Flexibles A/S. These super-hydrophobic surfaces with water-repelling structures provide rebound actions on the impacting droplets with the large contact angle θ. For the foils with the different micro- and nanostructures, the wetting properties are measured and impact with single droplet is presented. These coatings can be used for different engineering tasks, which need to establish and test new anti-icing/rain solutions for complex aerodynamic flows. We will start the present investigation from the initial point to include main aspects of the previous water-repellent investigations and test a single droplet impacts on the surface with the thermoplastic foil for the coating.

## INTRODUCTION

Erosion by raindrops is a frequent subject of concern being the destroyer of engineering structures. The impact of these interactions can be observed along all exterior solid surfaces in both nature and engineering. Today an intensive development of sustainable energy plants (on- and offshore wind farms etc.) offers an additional challenge for the anti-water erosion of immobile or rotating elements in their constructions on which surface firstly a significant water-film is usually formed by an intensive rain from the many droplets. The films also change the droplet blows impacting on the surface. Nevertheless, knowledge about the single droplet impacting on the wall has, of course, a basic role in studying the phenomena.

An adjoining problem to the water-erosion under our consideration in the review is the ice accretion inheriting the countries with the specific climatic conditions. The ice accretion on civil engineering structures represents a large problem to the safety and operation. For example, transmission lines can experience extreme high additional static loading due to massive ice accretion on the cable causing power blackouts. Telecommunication and meteorological equipment may suffer from ice accumulation or even fail. Larger pieces of the accreted ice fall off imposing a potential risk for serious or even fatal accidents of pedestrians around the building or for the traffic crossing the bridge. Apart

*International Conference on the Methods of Aerophysical Research (ICMAR 2018)*
AIP Conf. Proc. 2027, 030045-1–030045-11; https://doi.org/10.1063/1.5065139
Published by AIP Publishing. 978-0-7354-1747-2/$30.00

from increasing the mass and with that the dead weight of a structure, ice can alter the dynamic behavior and the dynamic excitation of a structure. Most current de-icing systems include either physical or chemical removal of ice, which is resource- and energy-intensive as well as environmentally polluting. A more desirable approach is to employ highly ordered super-hydrophobic materials to remove initial water droplets before the icing formation on a surface.

Last part of our consideration devotes to the central concept of the water-repellent surfaces which fabrications is inspired by nature. Indeed many exterior natural coatings of plant surfaces or animal skins contain complex 3D structures of different geometries on micro- or nanoscale to reduce the flow friction eliminating the water droplets on the surfaces with anti-erosion and de-icing effects. Many have attempted to repeat these natural structures in engineering by synthetic coatings with hydrophobic surfaces to reduce aerodynamic losses and erosion by the water-repellent effect. However, the successful natural solutions could not be profitably reproduced in many engineering tasks, dominatingly due to two main factors: a high cost of production of the surface coatings and a low wear resistance of the synthetic materials. Recent advances at DTU Nanotechnology have finally overcome these difficulties, opening up for the possibility of studying interactions of these wear-resistant coatings with both static and dynamic liquid flow interactions. Here we will estimate a perspective for the new technology with the superhydrophobic coating for many potential applications of Danish industries. The established hydrophobic and wear resistance properties of the nanostructured coatings will be compared with the characteristics of applications where a reduction of the friction losses and erosion is vital. Important examples include wind turbines, solar energy panels, offshore and ship constructions, highways, power lines, bridge and building constructions etc. The expected outcome is guidelines for utilization of surface coatings in different application technologies. However, we will start the present investigation also from the initial point of the knowledge including the single droplet impacting on the wall which has, of course, a basic role in studying the phenomena on the surface with the thermoplastic foil for the coatings.

## STATE OF THE ART IN STUDY OF DROP IMPACTS AND ICE ACCRETIONS

The Section is organized as follows. The next Subsection formulates the initial knowledge on the single droplet impacting with both dry and wetting walls. The second Subsection describes the problems when the continuous water films form under heavy rain condition on surfaces of the engineering structures. The last Subsection presents the results of the ice accretion for different conditions.

### A single droplet impacting on dry or wetting walls

A liquid drop colliding with a solid surface is associated with many phenomena: droplets can stick, spread, bounce (rebound), splash etc. Fig. 1 depicts some of the phenomena [1]. The study of the interactions of a droplet hitting a wall is well described in the literature (e.g. [2-6]).

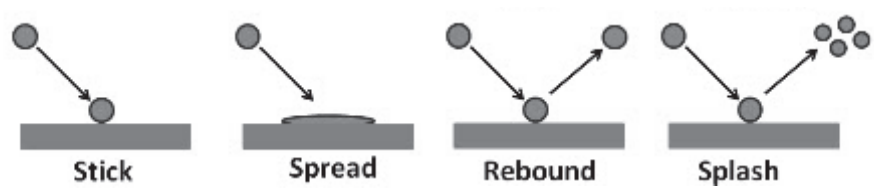


**FIGURE 1.** Sketch of main types of the wall interactions of the single droplet.

Although there is a great experimental progress on the droplet impact problem, a consensus has yet to be reached on many of its basic configurations, which morphology may take very complex forms (Fig. 2).

The outcome of drop impact depends on the impact velocity, its direction relative to the surface, drop size, the properties of the liquid (its density, viscosity, viscoelasticity, and some other non-Newtonian effects for rheologically complex fluids) the surface or interfacial tension, the roughness and wettability of the solid surface as well as on the non-isothermal effects (e.g., solidification and evaporation), and air entrapment. A drop may be spherical or elliptic (due to oscillations) at the moment of impact. It may impact on the free surface of a liquid in a deep pool, on a thin liquid film on a wall, or on a dry solid surface. The impact may be normal (perpendicular) or oblique (at an angle).

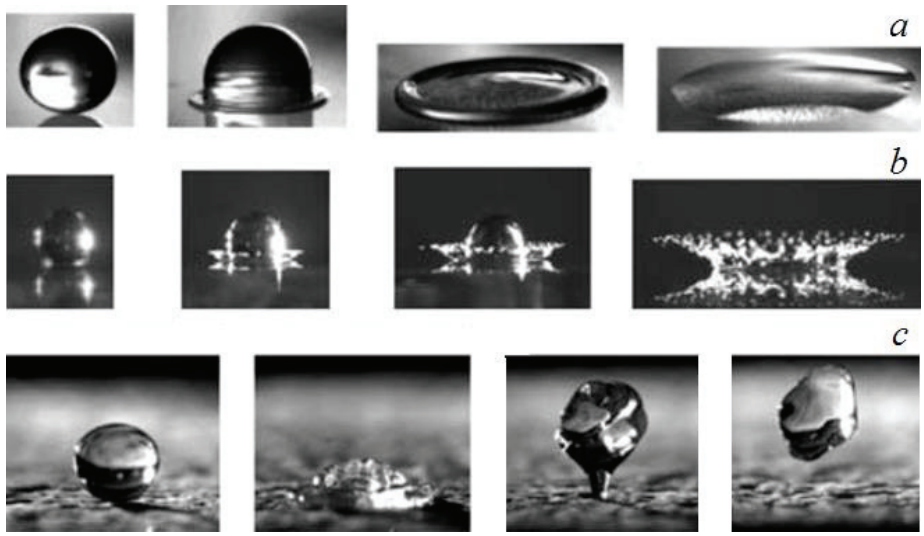


**FIGURE 2.** Examples of morphologies of drop impact on a dry surface: a) spread, b) splash and c) rebound [7].

The last review about the drop impact on a solid surface was published by Josserand and Thoroddsen [8] and we will follow their main conclusions. In this review, the authors focus on recent experimental and theoretical studies, which aim at unraveling the underlying physics of liquid inertia, viscosity, and surface tension etc. To define the different parameters involved in drop impacts, the authors considered as a prototype the normal impact of a spherical liquid drop on a flat solid substrate.

The drop diameter is $D = 2R$, and the normal impact velocity is $V$. The liquid and surrounding gas have densities $\rho_l$ and $\rho_g$, and dynamical (kinematic) viscosities $\mu_l$ ($\nu_l = \mu_l / \rho_l$) and $\mu_g$ ($\nu_g = \mu_g / \rho_g$), respectively. The surface tension is denoted by $\gamma$ and the gravity by g, which is oriented along the vertical direction. In general, the impact dynamics were first characterized by the Reynolds, Weber, and Ohnesorge numbers, defined with the liquid properties as

$$Re = \frac{\rho_l D V}{\mu_l}, \; We = \frac{\rho_l D V^2}{\gamma}, \text{ and } Oh = \frac{\mu_l V^2}{\sqrt{\rho_l D \gamma}}, \tag{1}$$

which balance the inertia with the viscous and the capillary forces, respectively.

To demonstrate a role of the introduced parameters (1) involved in drop impacts, we refer to [9]. In this work, the authors provide a comprehensive analysis of the parameter space of the impact problem. The main cross-section of this parameter space (the diameter–velocity sub-space) is reproduced in Fig. 3, a. The original overview of experimental works on droplet impact by Visser et al. [9] contains only industrial needs of spray/wall interactions in the coating, cleaning, cooling, and combustion. The industrial tasks dominate in them plot also because today inkjet droplets play an increasing role in fabrication, from the soldering of electronics to microarrays in biotechnology. In nature, nevertheless, a drop of water hollows stones or engineering structures causes their erosion during rain. Raindrops impact at their terminal velocity, which is greater for larger drops due to their larger mass to drag ratio. At sea level and without wind, 0.2-0.5 mm drizzle impacts at 1-2 m/s, while large 5-9 mm drops impact at around 9-30 m/s (with wind speed). An intensive building of on- and offshore wind farms offers an additional level of the raindrop impacts on rotating blades with tip velocities 100-150 m/s. These limits for the raindrops are extremely expanded of both cross-sections the impact problem, which was shown by new thick curves of Fig. 3.

Figure 3, b shows in terms of a dimensionless representation of the parameter space assuming the relevance of certain forces and processes (the Weber- and Reynolds numbers). The thin line indicates the separation between viscosity- and surface tension-dominated regimes (under versus above the line, respectively). Visser et al [9] explain the thin curve by the maximum spreading of the impacting droplet which is the result of the competition of forces. On the one hand, inertia forces drive the liquid to radial expansion. On the other hand, surface tension (capillary force) pulls back the expanding sheet, and viscosity (viscous force) dissipates part of the energy, limiting the maximum spreading size. The limiting cases, in which inertia forces are balanced by either surface tension or viscous dissipation, were separated by the parameter P = We/Re4/5 = 1 modeled by Clanet et al. [29]. Fig. 3, b does not indicate the existing droplet experiments for the P > 1, which can be used to obtain accurate predictions for the rain-scale

experiments by using scale-invariant of the existing data, although of course, it is not obvious that this scale-invariance must hold.

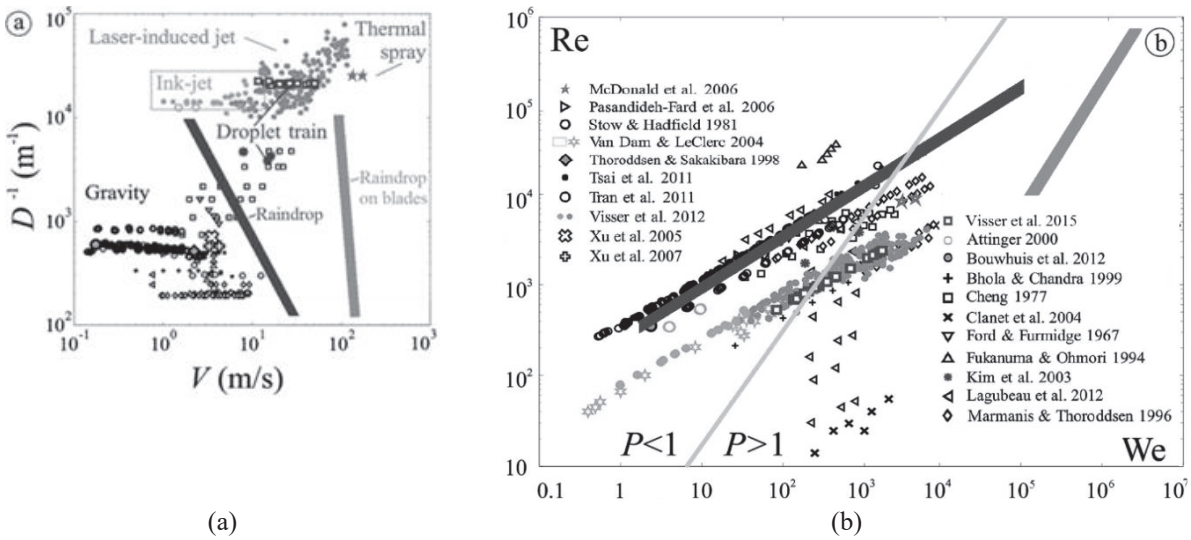


(a) (b)

**FIGURE 3**. Overview of experimental work on droplet impact showing the phase of inverse (in accordance with the review [9]): (a) diameter versus velocity and (b) the Reynolds number versus the Weber number (the plotted data by symbols was indicated in [9-29]). The P-line indicates the separation between viscosity - (P < 1) and surface tension - (P > 1) dominated regimes [9]. The thick lines show possible parameters of raindrops to the ground (black) and on blades of wind turbines (grey) – current data.

Finally, other dimensionless parameters can be present in the dynamics, often hidden in the literature, and related to the drop shape (e.g., the aspect ratio of the drop at impact) or the substrate properties, in particular, the contact angle θ and roughness distribution describing the hydrophobic properties and slip velocity $V_{slip}$ on the surface (Fig. 4). The slip velocity and contact angle usually are defined in experiments and have strong influence to set the scale-invariant roles.

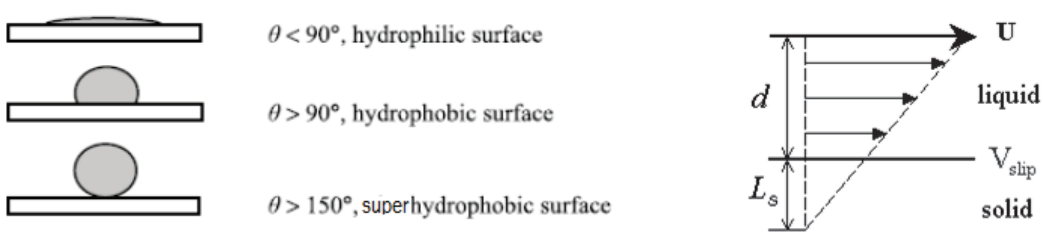


(a) (b)

**FIGURE 4**. Sketches of different types of the drop interactions (a) and slip velocity on the wall (b).

Later-time dynamics of the impact exhibit different behaviors depending on the impact and substrate parameters, ranging from smooth spreading to splashing, jetting, and rebound. In reality, only the spreading of drop impact has been expanded and described appropriately. In the novel investigation [30] the authors have studied different slip conditions and liquid-solid contact angles at the solid surface to show an important of the substrate properties (roughness and hydrophobicity under the same Re and We). They considered the limit cases with no-slip, $V_{slip} = 0$, and free-slip $V_{slip}$ = U (Fig. 4, b). For the free-slip case, they used both contact angle θ = 90˚ and 180. In the article was also investigated the energy budget and dissipation mechanisms during droplet impact on solid surfaces which can be employed to estimate of an erosion of solid surfaces in future. The authors have found an interesting fact, that for high impact velocities and negligible surface friction at the solid surface (i.e. free-slip case, $V_{slip}$ = U), approximately one-half of the initial kinetic energy is transformed into surface energy, independent of the impact parameters and the detailed energy loss mechanism.

In nature, unfortunately, the water drops during rain in atmospheric conditions follow splashing which usually describes aerosol phase with small bounced bubbles [31]. There have been many attempts to create the splashing theory [32-35] but all of them only apply for special cases and do not include the influence of different natural factors, e.g. the difficulty in distinguishing between the different aerosol phases (Fig. 2), or the surface wettability or roughness etc. Thus, an up-to-date parametric study separating the splashing of the impacting droplet is needed to complete the theoretical and numerical description of the complex phenomena.

Another well-known review on the topic on the impacting drops by Yarin [3] concluded that for normal impacts on a dry solid surface, full characterization of the effect of the surface texture, i.e., wettability and roughness, on the drop evolution, is still to be achieved, although several experimental data are already available in the literature. Modeling of normal drop impacts on a dry surface resulting in spreading and deposition is reliable, although there is still no complete agreement on the boundary conditions to be implemented at the moving contact line. The transition from the spreading to the stage, where the contact line is arrested, is also still incompletely understood and poses significant obstacles to reliable modeling. The consequences of oblique impacts on dry surfaces (a droplet colliding with the wall at an angle) are still insufficiently studied and understood.

The review by Yarin [3] also dealt with the droplet impacts on liquid surfaces or wettable walls. This water film should appear on the surface when subject to rain. Here we will pay your attention to the different effects of the water drops colliding with the liquid films. This section deals with the situation involving pre-existing liquid films, or films created by impacts of previous drops because a rain should strongly wet the surface. The additional non-dimension values of the dimensionless film thickness – $H = h/2R$ (Fig. 7) and $K = We*Oh^{-2/5}$ becomes also important parameters in the dimensionless group. The real pattern of drop splashing, in this case, looks too complicated for any theoretical tools except, the numerical ones, because both additional unknown film thickness $H$ and velocity $V$ appear (Fig. 5) of which should be found experimentally.

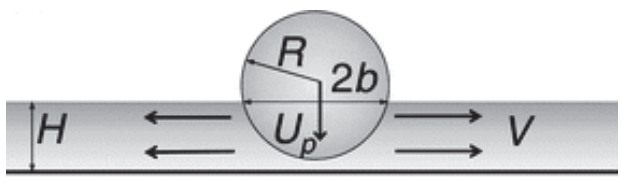


**FIGURE 5**. Sketch of the droplet interacting on the thin liquid film.

However, there are simple models based on a quasi-1D model [36], which can describe the thickness H and the crown position for a single impact on a thin pre-existing liquid layer. The authors of [37-39] generalized the simplest theory. The single-drop impacts on pre-existing films of the same liquid were experimentally studied by authors of [40-42]. These experiments revealed two characteristic flow patterns, like on the solid wall. At sufficiently low impact velocities the drops spread in the film under the wall, taking a visible outer rim. At still lower impact velocities practically no rim is visible, which termed deposition [42]. By contrast, at higher impact velocities the interaction took the shape of crowns consisting of a thin liquid sheet with an unstable free rim at the top (Fig. 8), from which numerous small secondary droplets were ejected [43]. Thus, both main forms, i.e. the splashing and spreading, of the impacting droplets appear here.

Yarin [3] concluded in his review that there is an understanding of the nature of the transition to splashing, crown formation, and propagation, for a normal drop impact on a thin liquid layer (less than the drop diameter), and that it is possible to model these phenomena. Transition to splashing after an oblique impact (a droplet colliding with an angle) still needs to be investigated, and models of crown propagation after such an impact still requires to be verified experimentally. Impacts on extremely thin liquid films, where the effect of the surface roughness cannot be disregarded, deserve more thorough examination.

## Airfoil and body aerodynamics in heavy rain

Rainfall on the immobile engineering structures and rotating blades of wind turbines (WT) should be considered just as an important meteorological factor as it is for aircraft. Indeed, adverse effects of rainfall on aircraft aerodynamic were a constantly hot subject in the meteorological aviation community for decades [44]. We try to separate the main factors of these influences, which can be applied to the rain erosion of the rotating WT blades and immobile structures.

Rainfall is a common physical phenomenon in people's life. Practical observation showed that the maximum raindrop diameter would not exceed 6 mm and the maximum falling velocity was approximately 9 mm/s without wind.

In order to conduct experimental investigations or develop analytical models on the effects of rain on aircraft aerodynamics, the characteristics of naturally occurring rainfall need to be understood. An understanding of the physics of raindrops is determined by analyzing various parameters, such as raindrop size distribution, the intensity of rain, the terminal velocity of a raindrop, the range of rainfall rate and the frequency of rainfall.

The literature on aviation comprehensively discussed the main detrimental influences of rain on aircraft. Figure 6 a)-d) shows the several aspects of them, which can be also important for the WT-blade aerodynamics:

- Rain erosion of the surface (aluminum alloy) [45]. The rain erosion of the blade is also the main problem for wind turbines.
- Rain-induced torque implemented on aircraft and the change in the center of pressure, which can produce a change in the balance of the WT-rotor rotation.
- Possible destabilization effect of water vapor condensation on airfoil boundary layer [46].
- Premature trailing edge separation for NACA64-210 airfoil in the rainfall condition at an angle of attack of 12-14 [47].

All factors mentioned in Fig. 6 for aircraft should also impact on the aerodynamics of the WT-blades but there is a significant difference between them concerning with the angle of the rainfall which is about the same for the wings and can be arbitrary for the rotating blades. Another potential detrimental influence of the water film is the water film separation occurring over the airfoil somewhat aft of the minimum pressure area, as shown in Fig. 10, b. The water film separates a sheet interacting with the airflow over the airfoil and deflecting the free-stream air up thus encouraging separation.

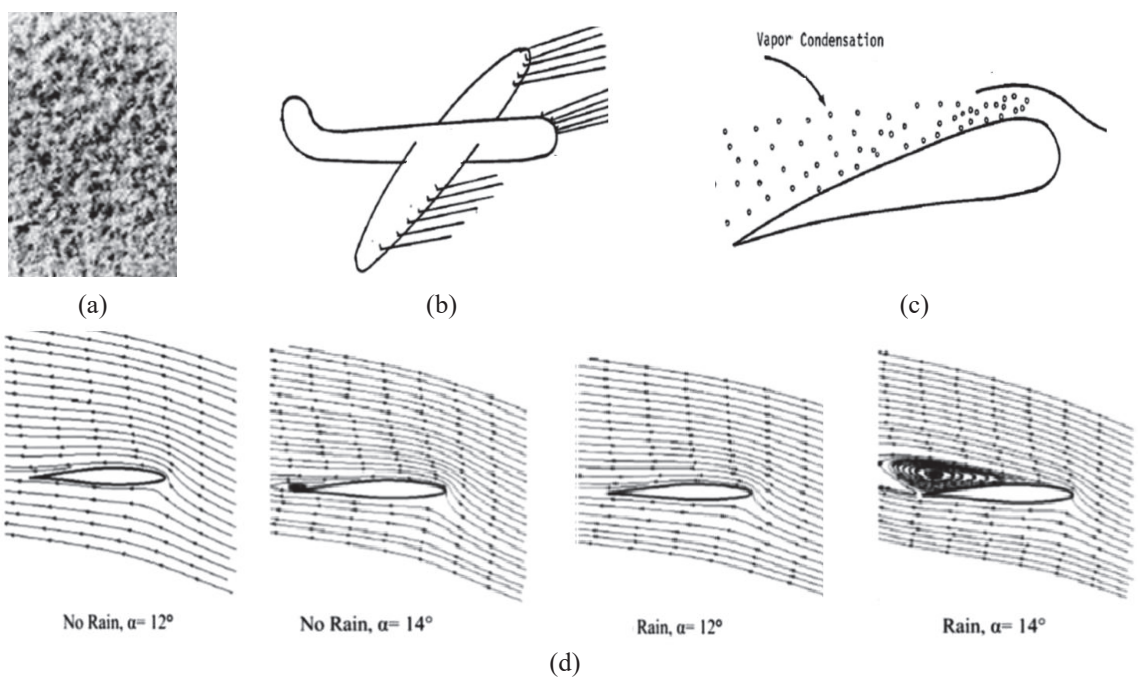


**FIGURE 6**. The main influences of rain on aircraft, which also can play a critical role in WT operation: (a) surface erosion; (b) tracts of the raindrop; (c) vapor condensation; (d) streamlines under different conditions [48].

According to published literature in the last decades, the following aspects has been investigated on the effects of rainfall on aircraft: aerodynamic performance degradation [48], raindrop trajectory [49], rain-affecting mechanisms, flight dynamic performance in heavy rain conditions [48, 50], and surface water film flowing characteristics [51, 52]. All these results are open studies on WT operation in rain conditions because the blade rotation makes a possibility of any rain direction for the airfoil surface.

Next question for the future studies is to test the lotus effect at the heavy rain condition. While single drop impact studies have been conducted amply in the past, testing of more practical and complex flow situations, including reduced flow resistance still remains an open yet industrially and academically important area of the study of the aerodynamics in heavy rain for mobile and moving different engineering structures.

## Ice accretion for different atmospheric conditions

The relevance of the icing problem is determined by the specific climatic conditions in the Arctic countries in which a control of the ice accumulation is important. The ice accretion on civil engineering structures represents a large problem to the safety and operation. Larger pieces of the accreted ice fall off imposing a potential risk for serious or even fatal accidents of pedestrians or for the traffic crossing around the building, bridge [53]. Other cases where ice accumulation imposes potential risks for operation, safety and erosion are: wind turbines operations in cold conditions, solar panels etc. (see Fig. 7)

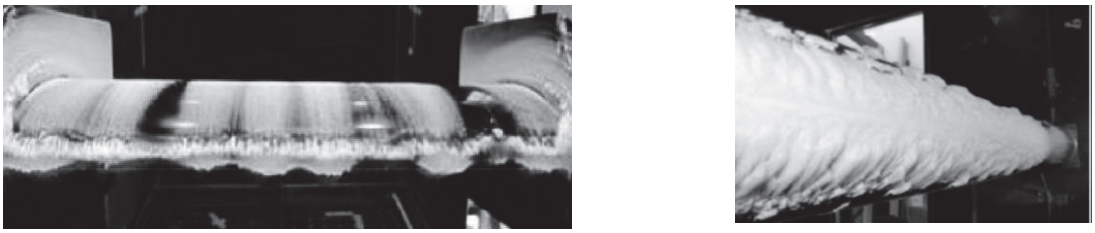

(a) (b)

**FIGURE 7**. Examples of the icing on (a) – a WT-profile [54] and (b) – a cable [53].

The effect of icing should be considered during the design process, including safety assessment, anti-erosion, and economic evaluation. Also, the effect of icing on the rotor aerodynamics should be considered since this may change the load distributions and dynamic responses. For stall-regulated wind turbines, icing can make the blades stall earlier than intended. Additional mass on the blade due to icing yields higher inertia forces on the rotor and may change the natural frequencies of the blade that should be considered during fatigue lifetime assessment of the structure. Possible ice throw from the wind turbines operating under ice condition is an important issue for wind farms near populated areas such as a ski resort or farmlands [54].

A modern solution to the anti-icing problem should include, but are effectively not limited to the following statements:

1. The ice-phobic material has to reduce significantly ice and snow build-up.
2. The material has to be inexpensive and environmentally friendly.
3. The ice-phobic material should be easily manufactured and applied as a coating of a bulk material to be used for both fabricated and new constructions.
4. This material has to withstand weather conditions of the coast at 0-300 m above sea level in the Arctic and it should be tested under realistic environmental conditions, for example in an icing wind tunnel at sufficiently high airspeeds to match the conditions encountered in nature.

# ANTI-WETTING AND DE-ICING BY SUPER-HYDROPHOBIC STRUCTURES

Production of new engineering materials with super hydrophobic properties is inspired by nature, where many plants grow water-repellent structures on their surfaces, consisting of complex 3D micro and nano-papillae [47]. Superhydrophobic surfaces are a popular solution for research on the de-icing. A number of studies freezing of water droplets on cooled super-hydrophobic surfaces have been carried out on samples of relatively expensive components, such as microstructured fluorinated Si, Al or Gold Thiols [55,56]. However, these successful solutions are hard to profitably reproduce in many engineering tasks due to a high cost of production of such surface coatings.

## Fabrication of superhydrophobic surfaces in thermoplastic foils

In order to scale up the production of superhydrophobic surfaces, the structures made in semiconductor materials or metals can be transferred into plastic via imprint. Nowadays there are multiple imprint platforms available, and the development is leaning towards roll-to-roll production of the structured surfaces. One of the examples of a successful roll-to-roll platform is R2R extrusion coating. This process has a high throughput and a potential for production of 2m wide foils at a speeds of up to 1000 m/min [57]. A schematics of the process is presented in Fig. 8, a. The melted polymer is pressed between two cylinders, hereby connecting with the carrier foil. The micro and nano-structured

molds are introduced at the cooling roller, where the polymer is cooled down and undergoes pressure, which results in the transfer of the pattern from the molds onto the foil.

The extrusion coating process is a well-established method for manufacturing of packaging foils. Introducing the micro and nano-structures into surfaces of thermoplastic polymers that increase the surface roughness, can change wettability properties and increase hydrophobicity. Such superhydrophobic thermoplastic foils can be used to prevent corrosion, improve aerodynamics or add self-cleaning properties to the material, as well as icing and rain protection of different aerodynamic constructions.

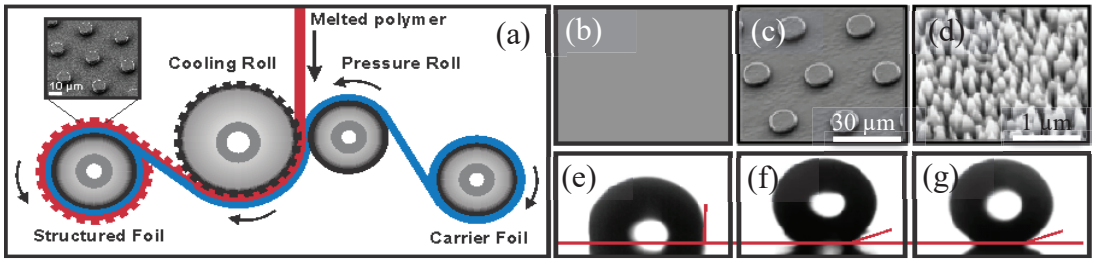


**FIGURE 8.** (a) A sketch of the Roll-to-Roll Extrusion Coating process: the structured molds are attached to the "Cooling Roll", where the melted polymer is brought into contact with the mold using the "Pressure Roll". It is possible to structure sheets up to 2 m in width. (b), (c), (d) Represent the investigated structures and (e), (f), (g) represent the respective contact angle measurement. (b) Flat PP surface, (c) micropillars, (d) nano-needles.

Multiple parameters determine the functionality of the produced foils: first of all, the yield of the pattern transfer (how much the produced structures resemble the intended structure in the mold). Secondly, the shape and size of the intended structure. Additionally, the type of the extruded polymer and lastly, the test and handling conditions. The high yield of the pattern transfer is important in order to achieve the consistent quality of the foils and provide a stable performance. The yield of the pattern transfer has been investigated for both micro- and nano-structures [57, 58] where good results for structures of the sizes between 100 µm down to 50 nm have been presented.

The hydrophobic effect in foils produced with the R2R EC has been demonstrated by Telecka et al [59]. Hydrophobicity is determined by the structure type and size. In Fig. 8 different shapes of structures are shown for PP foils (b,c,d) and the respective contact angles are presented in (e,f,g). For a flat PP surface the water contact angle is measured to be 102°±1°. Structuring the surface with a micropillar pattern changes the contact angle to above 150°; an array of nano-sized randomly distributed nano-needles (so-called nano-grass) further improves the water contact angle to exceed 160°. The contact angle hysteresis (difference between the advancing and receding angle at roll-off) is below 10° for the nano-grass structures, which makes these samples superhydrophobic. The superhydrophobic structures are inspired by the surface structures produced by several plants and animals, the so-called lotus effect. In Fig. 9 a, b an SEM image of the surface of a lotus flower is shown and a droplet resting on the surface, as measured by Wijesena et al [60]. A superhydrophobic polymer surface is presented in Fig. 9, c, d. The artificial water-repelling structure's rebound actions on the impacting droplets resemble the Lotus effect in the natural plants.

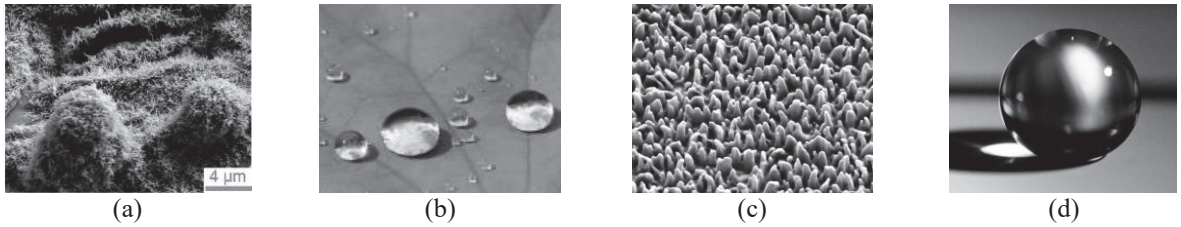


**FIGURE 9.** (a) Super-hydrophobic surface of a lotus leaf [61]; (b) droplet of water on the leaf demonstrating the Lotus effect [61]. (c) Super-hydrophobic surface created in a lab, mimicking the lotus-leaf structure; (d) a droplet of water on an artificial superhydrophobic surface (Photo by Jesper Scheel)

A water droplet impacting the flat PP foil does not achieve a full rebound, as it stays pinned to the surface (Fig. 10, a). The superhydrophobic nano-grass structures provide the total rebound at an impact with a similar water droplet (Fig. 10, b), demonstrating the Lotus effect and proving the superhydrophobicity. Different polymer types

would show different results, depending on the initial contact angle with water. This effect should be optimized in terms of durability of the surfaces versus the surface properties of the polymer.

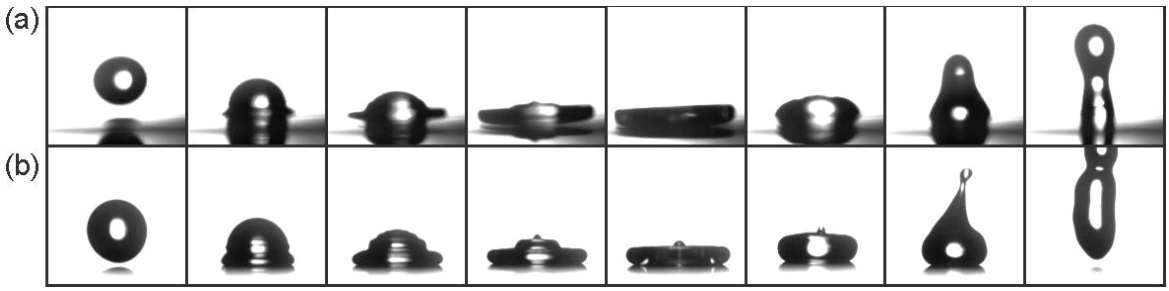


**FIGURE 10.** (a) A water droplet landing on an unstructured PP surface. (b) A water droplet landing on a nano-structured foil produced using a roll-to-roll extrusion coating process. The droplet stays pinned to the flat PP surface, at the same time the superhydrophobic structures provide the total rebound of the droplet.

The presented results should be used to define and design optimal super-hydrophobic surfaces among the different micro- and nanostructured patterns. These data can be used for further testing the existing and new theoretical and empirical models of heterogeneous nucleation. Furthermore, this investigations should deal with the study of how complex aerodynamic flows (Fig. 6, d) that may change the hydrophobic properties of the polymer foils, as the previous studies have only been dealing with interaction of the resting or free-falling droplets on super-hydrophobic surfaces.

## Further studies of the anti-wetting and de-icing properties of the thermoplastic foils

This high-speed and low-cost method looks very promising, however, the present investigation started only from an initial point to test a single droplet impacts on the surface with the thermoplastic foil for the coatings. These coatings can be easy to use for the different engineering tasks, which need to establish and test new anti-icing/rain solutions in the complex aerodynamic flows to include main aspects of the previous water-repellent investigations as an effective de-icing technique.

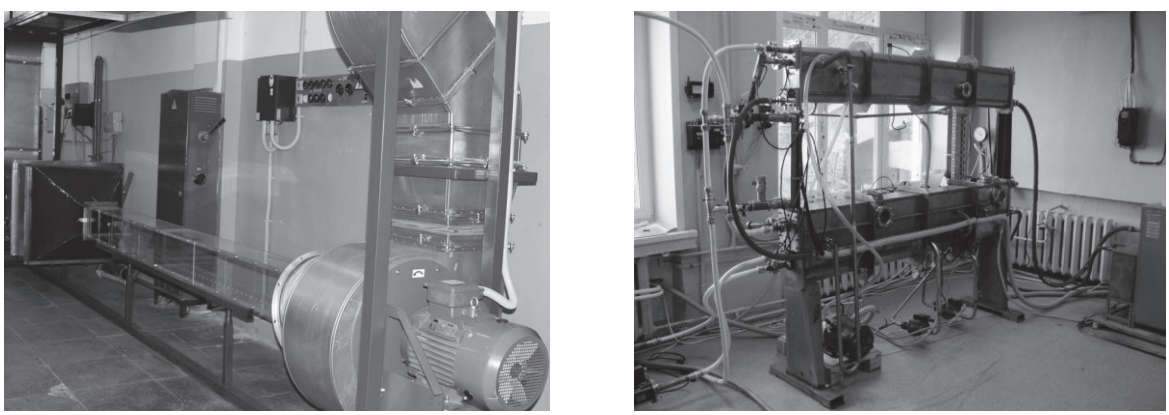

(a) (b)

**FIGURE 11.** (a) Wind tunnel and (b) Absorptive bromide-lithium refrigerator [64].

In next investigations, it should be studied how realistic flows around basic aerodynamic bodies and rotor blades influence the surface contact time and the contact area of impinging water droplets for the different super-hydrophobic coatings. The testing aerodynamic profiles [62] with the foil coating should be studied under realistic environmental conditions in a climatic wind tunnel at sufficiently high airspeeds and low temperature to match the conditions encountered in nature. The climatic conditions in the laboratory tests are provided by the combination of a wind tunnel and an absorptive bromide-lithium refrigerator (Fig. 11). Measuring techniques, including non-intrusive optical systems (high speed cameras, LDA, PIV), in combination with rapid prototyping techniques (3-d printing) for fast and

accurate manufacturing of geometrically complex test section elements [63], will be used to study the icing processes under various external conditions.

## CONCLUSION

In the current investigation, we described the state of the art in the study of anti-rain and de-icing which unfortunately restricts by the tests of the single droplet. Later-time dynamics of the impact exhibit different behaviors, depending on the impact and substrate parameters, ranging from smooth spreading to splashing, jetting, and rebound. In practice, only the spreading of impacting drops has been expanded and described appropriately. For the more complex cases (splashing, jetting, rebound, spray etc.), an up-to-date parametric study separating in the splashing of the impacting droplet is needed to create appropriate theories.

Moreover, the understanding of the nature of the transition to splashing, crown formation, and propagation, for a normal drop impact on a thin liquid layer (less than the drop diameter) has been presented in literature and shown to be modeled by relating simple models. Unfortunately, the consequences of oblique impacts on dry surfaces (a droplet colliding with the wall at an angle) and on wetted surfaces are still insufficiently studied and understood. Thus, the typical situation when droplets impact at an angle on the blade surface has not been solved still!

The raindrop conditions have extremely expanded the limits for of the impact problem, which were early studied for the industrial needs of mm-size spray/wall interactions in the coating, cleaning, cooling, combustion and new material fabrication. Many successful results of the airfoil of the aircraft should be expanded at the blades of WT operating at strong rain or icing conditions because the turbine rotation makes a possibility of any rain and snow directions causing at the airfoil surface.

In the current review as a new idea, it was suggested for aerodynamic bodies and WT blades protection against the water/ice erosion to use coating based on the thermoplastic polymer in order to exploit the lotus effect. In practice, this can be accomplished by using new manufacturing technique as that was proposed by DTU and Danapak Flexibles A/S and can be easy to use. This original approach may open up ways for the current and new applications using the anti-erosion superhydrophobic coating for which the testing should continue to be an active research area in both its experimental and theoretical aspects several next years. Next question for the future studies is to test the lotus effect also at the heavy rain and icing conditions in the climatic wind tunnels.

## ACKNOWLEDGMENTS

This work was supported in part by the Innovation Fund Denmark through the project XNano (grant no. 4135-00142B) and RScF (grant no. 14-19-00487).

## REFERENCES

1. J. Mutyal, http://www.ansys-blog.com/accurate-spray-wall-interaction-predictions-ansys-fluent-16-0/ (2015).
2. M. Rein, Fluid Dyn. Res. **12** (2), 61–93 (1993).
3. A. L. Yarin, Annu. Rev. Fluid Mech. **38**, 159-192 (2006).
4. M. Marengo, C. Antonini, I. V. Roisman and C. Tropea, Curr. Opin. Colloid Interface Sci. **16(4)**, 292–302 (2011).
5. D. Quere, Annu. Rev. Fluid Mech. **45**, 197–215 (2013).
6. S. T. Thoroddsen, T. G. Etoh, and K. Takehara, Annu. Rev. Fluid Mech. **40**, 257–285 (2008).
7. R. Rioboo, C. Tropea, and M. Marengo, Atm. & Sprays **11**, 155–165 (2001).
8. C. Josserand and S. T. Thoroddsen, Annu. Rev. Fluid Mech. **48(1)**, 365–391 (2016).
9. C. W. Visser, P. E. Frommhold, S. Wildeman, R. Mettin, D. Lohse, and C. Sun, Soft Matter **11**, 1708-1722 (2015).
10. A. McDonald, M. Lamontagne, C. Moreau and S. Chandra, Thin Solid Films **514**, 212-222 (2006).
11. M. Pasandideh-Fard, Y. M. Qiao, S. Chandra and J. Mostaghimi, Phys. Fluids **8**, 650-659 (1996).
12. C. D. Stow and M. G. Hadfield, Proc. R. Soc. A **373**, 419-441 (1981).
13. D. B. van Dam and C. Le Clerc, Phys. Fluids **16**, 3403-3414 (2004).
14. S. Thoroddsen and J. Sakakibara, Phys. Fluids **10**, 1359-1374 (1998).
15. P. Tsai, R. C. A. van der Veen, M. van de Raa and D. Lohse, Langmuir **26**, 16090-16095 (2010).
16. T. Tran, H. J. J. Staat, A. Prosperetti, C. Sun and D. Lohse, Phys. Rev. Lett. **108**, 036101 (1-5) (2012).

17. C. W.Visser, Y.Tagawa, C. Sun and D. Lohse, Soft Matter **8**, 10732-10737 (2012).
18. L. Xu, L. Barcos and S. Nagel, Phys. Rev. E: Stat., Nonlinear, Soft Matter Phys. **76**, 066311 (2007).
19. L. Xu, W. Zhang and S. Nagel, Phys. Rev. Lett. **94**, 184505 (1-4) (2005).
20. D. Attinger, Z. Zhao and D., J. Heat Transfer **122**, 544-556 (2000).
21. W. Bouwhuis, R. C. A. van der Veen, T. Tran, D. L. Keij, K. G. Winkels, I. R. Peters, D. van der Meer, C. Sun, J. H. Snoeijer and D. Lohse, Phys. Rev. Lett. **109**, 264501 (2012).
22. R. Bhola and S. Chandra, J. Mater. Sci. **4**, 4883-4894 (1999).
23. L. Cheng, Ind. Eng. Chem. Process Des. Dev. **16(2)**, 192-197 (1977).
24. R. E. Ford and C. G. L. Furmidge, "Impact and spreading of spray drops on foliar surfaces," in *Wetting*, (Soc. Chem. Industry Monograph **25**, 1967), p. 417.
25. H. Fukanuma and A. Ohmori, "Behavior of molten droplets impinging on flat surfaces" In *Proc. 7th National Thermal Spray Conference*, (ASM International, Boston, MA, 1994), pp. 563–568.
26. H.-Y. Kim, S.-Y. Park and K. Min, Rev. Sci. Instrum. **74**, 4930-4937 (2003).
27. G. Lagubeau, M. A. Fontelos, C. Josserand, A. Maurel, V. Pagneux and P. Petitjeans, J. Fluid Mech. **713**, 50-60 (2012).
28. H. Marmanis and S. T. Thoroddsen, Phys. Fluids **8**, 1344-1346 (1996).
29. C. Clanet, C. Beguin, D. Richard and D. Quere, J. Fluid Mech. **517**, 199-208 (2004).
30. S. Wildeman, W. Visser, C. Sun, D. Lohse, J. Fluid Mech. **805**, 636-655 (2016).
31. Y.S. Joung and C.R. Buie, Nat. Commun. **6**, 6083 (1-9) (2015).
32. L. Duchemin, C. Josserand, C. R. Mec. **340**, 797–803 (2012).
33. S. Mandre and M. P. Brenner, J. Fluid Mech. **690**, 148–172 (2012).
34. J. Palacios, J. Hernandez, P. Gomez, C. Zanzi and J. Lopez, Exp. Therm. Fluid Sci. **44**, 571–582 (2013).
35. G. Riboux and J. M. Gordillo, Phys. Rev. Lett. **113**, 024507 (2014).
36. A. L. Yarin and D. A. Weiss, J. Fluid Mech. **283**, 141–173 (1995).
37. M.F. Trujillo and C.F. Lee, Phys. Fluids **13**, 2503–2516 (2001).
38. I.V. Roisman and C. Tropea, J. Fluid Mech. **472**, 373–397 (2002).
39. A. I. Fedorchenko and A. B. Wang, Phys. Fluids **16**, 1349-1365 (2004).
40. G. E. Cossali, A. Coghe and M. Marengo, Exp. Fluids **22**, 463–472 (1997).
41. A. B. Wang and C. C. Chen, Phys. Fluids **12**, 2155–2158 (2000).
42. R. Rioboo, C. Bauthier, J. Conti, M. Voue and J. De Coninck, Exp. Fluids **35**, 648–652 (2003).
43. M. Rieber and A. Frohn, Int. J. Heat Fluid Flow **20**, 455–461 (1999).
44. Y. Cao, Z. Wu and Z. Xu, Prog. Aerosp. Sci. **71**, 85–127 (2014).
45. A. A. Fyall, Philos. Trans. R. Soc. Lond. Ser A Math. Phys. Sci. **260** (1110), 161–167 (1966).
46. J. K. Luers, AIAA Paper **83-0206** (1983).
47. R. Zhang and Y. Cao, J. Aerosp. Power. **25** (9), 2064–2049 (2010).
48. Z. Wu and Y. Cao, Aeronaut. J. **118**, 643–668 (2014).
49. J. R. Valentine and R. A. Decker, J. Aircraft **32**, 100–105 (1995).
50. Z. Wu and Y. Cao, Int. J. Multiphase Flow **69**, 81–92 (2015).
51. E. C. Hastings Jr. and L. M. Weinstein, NASA-TM-**85796** (1984).
52. E. C. Hasting and G. S. Manuel, AIAA Paper **85-0259** (1985).
53. C. Demartino, H. H. Koss, C. T. Georgakis and F. Ricciardelli, J. Wind Eng. Ind. Aerodyn. **138**, 98–119 (2015).
54. M. Etemaddar, M. O. L. Hansen and T. Moan, Wind Energy **17**, 241-265 (2014).
55. L. Mishchenko, B. Hatton, V. Bahadur, J. Taylor, T. Krupenkin and J. Aizenberg, ACS Nano **4(12)**, 7699-7707 (2010).
56. D. K. Sarkar, M. Farzaneh, J. Adhes. Sci. Technol. **23**, 1215–1237 (2009).
57. S. Murthy, M. Matschuk, Q. Huang, N. K. Mandsberg, N. A. Feidenhans'l, P. Johansen, L. Christensen, H. Pranov, G. Kofod, H. C. Pedersen, O. Hassager and R. Taboryski, Adv. Eng. Mater. **18** (4), 484-489 (2016).
58. N. Okulova, P. Johansen, L. Christensen and R. Taboryski, MEE **176**, 54-57 (2017).
59. A. Telecka, S. Murthy, L. Schneider, H. Pranov and R. Taboryski, ACS Macro Lett. **5**, 1034−1038 (2016).
60. R. Wijesena, "How lotus leaf make water droplets dance on its surface," (http://ninithi.com/ , July 30, 2015).
61. E. Soegaard, "Injection molded self-cleaning surfaces," Ph.D. thesis, DTU Nanotech, 2014.
62. V. Okulov, Thermophys. Aeromech. **25** (1), 1-20 (2018).
63. I. Litvinov, S. Shtork, E. Gorelikov, A. Mitryakov and K. Hanjalic, Exp. Therm. Fluid Sci. **91**, 410-422 (2018).
64. K. I. Stepanov, D. G. Mukhin, S. V. Alekseenko, O. V. Volkova, Thermophys. Aeromech. **22(4)**, 481–489 (2015).